

On the physics of material processing with femtosecond lasers

Ingolf V. Hertel,^{*1,†1} Razvan Stoian,^{*1} David Ashkenasi,^{*1,†2} Arkadi Rosenfeld,^{*1} and Eleanor E. B. Campbell^{*2}

^{*1} Max Born Institute, Germany

^{*2} Department of Experimental Physics, University of Gothenburg and Chalmers University of Technology, Sweden

Ultrashort pulsed laser ablation of dielectrics has been investigated using ex-situ morphological examinations in combination with *in-situ* time-of-flight mass spectrometry of the ablated species. Analysis of the energy spectrum of the ablation products provides a wealth of information on the processes occurring during femtosecond laser ablation of materials. The presentation will focus on the case of sapphire (Al_2O_3) and discuss the fundamental processes in ultrashort pulsed laser sputtering. Two different ablation phases have been identified, a “gentle” phase with low ablation rates and a “strong” etch phase with higher ablation rates, but with limitation in the structure quality. A comparison of the energy and momentum distributions of ejected ions, neutrals, and electrons allows one to distinguish between non-thermal and thermal processes that lead to the macroscopic material removal. Fast positive ions with charge-scaled momenta are resulting from Coulomb explosion of the upper layers at low fluence and low number of irradiating laser pulses (“gentle” etch phase). Pump-probe studies with fs laser pulses reveal the dynamics of excitation and electron-mediated energy transfer to the lattice. At higher laser fluences or after longer incubation, evidence for phase explosion can be derived from both the morphology of the surface and the results of the *in-situ* experiments.

Introduction

Improved availability and compactness of ultra-short, sub-ps pulsed solid state lasers has stimulated a growing interest in the exploiting of the enhanced flexibility of femtosecond-technology for micro-machining. Disregarding price and user friendliness of present laser systems – which will improve massively in the coming years – ultra-short laser pulses offer a variety of advantages for precision micro-fabrication. Presently, the first designated commercial femtosecond machining stations are available for an expanding market. Due to lower energetic thresholds for sub picosecond ablation and the controllability of individual laser pulses (*e.g.* by laser pulse length) the amount of energy deposited into the processed sample can be minimized and highly localized. This leads to a reduction of unwanted thermal effects, a minimization of energy diffusion, and little debris (bulk material ejection) so that very clean microstructures can be achieved with pulses optimized for the individual application. Figure 1 illustrates as an example that the most perfect micropores can be achieved with 800 nm, 200 fs pulses in *c*- Al_2O_3 (sapphire) – while other materials, *e.g.* CaF_2 may well require picosecond treatment for optimal results.¹⁾ Also non-linear optical effects may be exploited: efficient multi-photon absorption allows one to modify transparent materials even inside the bulk and to obtain sub-wavelength structure sizes. Self-focusing due to the non-linear optical Kerr effect may be used to induce long, narrow 3D-modification traces into the bulk of wide band-gap materials. Long, micrometer thin channels can be also drilled taking advantage of the high ablation rates and low heat deposition when employing ultrashort laser pulses.²⁾

These prospects warrant a detailed understanding of the physical mechanisms involved in material processing with ultrashort laser pulses. From the view point of basic research, subpicosecond pulses offer additional advantages: In contrast

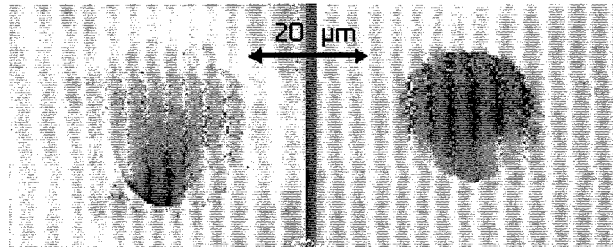


Fig. 1. Micropores in sapphire created with ultrafast 800 nm laser pulses illustrating the influence of pulse duration (left 4.5 ps, right 200 fs – same laser fluence).

to the more standard investigations of material ablation, or sputtering, with ns laser pulses, they do not interact with the plume of ablated material since the pulse has stopped before the material removal takes place. The avoidance of secondary effects due to plume heating as well as the possibility of pump-probe experiments on a time-scale of some tens of femtoseconds to some hundreds of picoseconds makes a detailed investigation and understanding of the laser-matter interactions, energy dissipation and mechanisms of material removal feasible. In addition, new avenues are opened to a basic understanding of energy deposition into the sample and to a real time monitoring of the electronic and atomic processes in solids under the ultrashort pulsed laser excitation.

The present study focuses mainly on sapphire (*c*- Al_2O_3) in view of its many useful mechanical, optical and electrical properties, and also since it shows in a very clear manner two distinctively different ablation phases which are believed to be characteristic for pulsed laser structuring of wide band-gap materials.^{3,4)} A “gentle” phase is found for low laser fluences (and low numbers of laser shots) which is characterized by the removal of a few nm (20–30 nm) in depth per laser shot, leaving behind a smooth surface. Surface charging and ion Coulomb explosion is found responsible. The “strong” phase is characterized by an order of magnitude higher abla-

^{†1} e-mail address: hertel@mbi-berlin.de

^{†2} Present address: LMTB, Berlin-Adlershof, Germany

tion rate per pulse. It is accompanied by significant plasma light emission and shows a violent expulsion mechanism tentatively assigned to phase explosion. We use:

- a quantitative ex-situ evaluation of ablation results (AFM, SEM, optical microscope),
- *in-situ* determination of the velocity distribution of ablation products,
- and pump-probe techniques,

to quantify the appearance of the two phases and glean evidence on the mechanisms and dynamics of the processes involved. The laser pulses as such offer a convenient tool to probe the energy deposition and modification process of the material in very controlled manner. The parameters that we vary are:

- number of pulses/site: N
- pulse duration: τ [ps, fs]
- laser fluence: F [J/cm^2]
- and in the pump-probe experiments delay time: Δt .

Our study is guided by the generally accepted picture for the excitation of dielectrics with ultrashort, near infrared or visible laser pulses: The initiating excitation mechanism is believed to be multi-photon absorption, either from already present morphological or structural defect states in the band gap or by interband transitions, which seed free electron heating and additional ionization due to electron impact.⁵⁾ This is followed by photoelectron emission with surface charging and thermalisation of the quasi-free electronic system on a material-dependent time-scale and energy transfer to the lattice by electron-phonon coupling with subsequent heating of the sample. The questions we have tried to answer refer to how and how long does it take for a particle to be emitted and the approach was to identify the paths and temporal characteristics of the energetic channels originating from the laser beam and coupled with the emitted particle itself. What is the energetic spectrum of the emitted particles? What happens to the surface and to the affected bulk after laser irradiation? To what extent can this micron or sub-micron modification be controllable by an optimal choice of laser parameters? What is the role of laser induced defects in surface micro-machining or in the optical properties of the irradiated solid?

Quantitative ex-situ identification of gentle and strong ablation phase

It will be shown that a suitable choice of laser parameters can tune the transition between different processes, dominated by either non-thermal or thermal mechanisms, respectively. A first fingerprint of this change in mechanisms is gleaned from determining the material removed by a single, ultra-short laser pulse as function of fluence. This is shown in Fig. 2 for sapphire at a pulse width of 100 fs as determined by a careful evaluation of the volume of the ablated spot by Atomic Force Microscopy (AFM). At low fluence, it shows in a log-log plot a high slope of ≈ 8 , indicative of a high order excitation. At high fluence we observe a nearly linear increase, *i.e.* the material removal is proportional to incident energy which reflects a thermal process and significant temperature rise of the lattice.

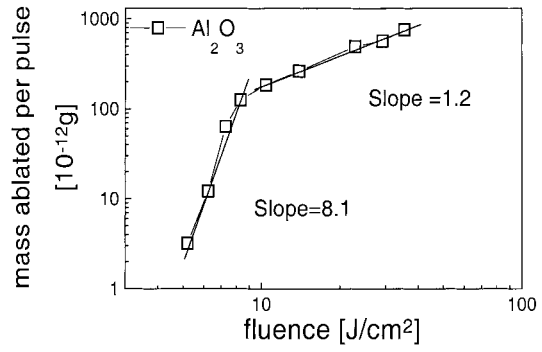


Fig. 2. Log-log plot of the amount of material removed from $c\text{-Al}_2\text{O}_3$ after the first laser pulse (800 nm, 100 fs) as function of its fluence.

This change of mechanisms which is attributed to different ablation phases is most evidently identified by the visual appearance of the irradiated area in a scanning electron microscope (SEM). This is illustrated in Fig. 3 for different number of shots per site at constant fluence. The first laser shots above the damage threshold initiate the *gentle etch-phase*. For 200 fs irradiation the gentle etch-phase ($N < 30$) is characterized by an extremely smooth surface (sometimes even smoother than the initial state), both at the sidewall and at the bottom of the dip with almost no pattern developing except ripples²⁾ and with no debris particles around the rim. Material is removed with every laser pulse, including the first one. The ablation rate is low, around 20–30 nm/pulse as determined by a volume evaluation using AFM.⁴⁾

At a higher number of laser pulses, the appearance of the spot changes dramatically as illustrated for $N = 30$ in Fig. 3. The surface shows the characteristics of the strong ablation phase: increased roughness and signs of a violent process of thermal nature, among them droplets, melting traces and splintered edges. At a still higher number of shots even crater formation is observed. The mechanisms underlying this *strong etch phase* is basically thermal and may be associated with phase explosion.^{6,7)}

The change from the gentle to the strong etch-phase occurs between 25 and 30 laser pulses per site at this particular fluence and depends also on fluence and laser pulse-width. At the same time the ablation rate increases drastically (≈ 300 nm/pulse). This allows us to determine the crossover between the two phases in a quantitative manner⁸⁾ as illustrated in Fig. 4 (upper panel). We can also determine the degree of ionization in the plume from a quantitative evaluation of the ion current during each shot and comparison with the amount of material ejected. As seen in the lower

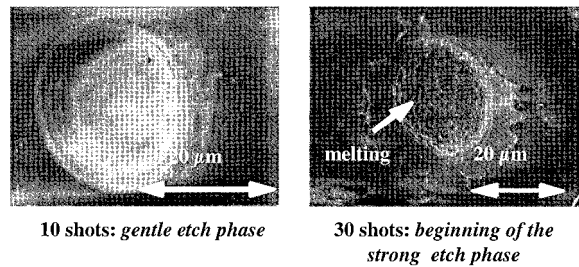


Fig. 3. Transition from gentle to strong etch phase in $c\text{-Al}_2\text{O}_3$.

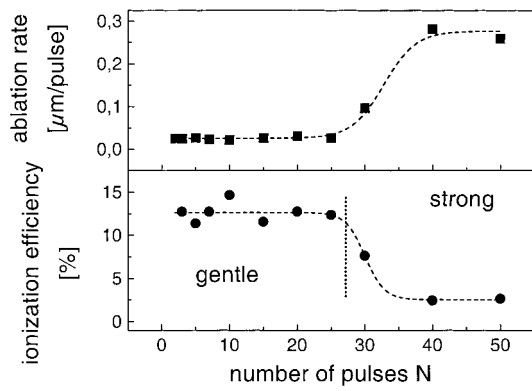


Fig. 4. Quantitative determination of the transition from gentle to strong etch phase by measuring the ablation rate per laser pulse and the degree of ionization in the plume as a function of the total number of laser pulses N applied to a given site. The pulse duration was $\tau = 200$ fs, the laser fluence $F = 4.0$ J/cm².

panel of Fig. 4, the ionization efficiency also changes dramatically when the ablation changes from gentle to strong: in this case, the degree of ionization drops massively. It should be noted that the results of these measurements are not dependent on the repetition rate at which the laser is operated (on sub-Hz and Hz scale).

We attribute these dramatic changes observed as a given site is exposed to a number of laser shots to the build up of defect sites by each laser shot. We clearly observe incubation as discussed in the introduction.

The measurements described above were taken at a fluence of 4 J/cm², just above the single shot ablation threshold (3.5 J/cm²). In addition, the incubation effects manifest themselves also in a visible reduction of the ablation threshold at repetitive irradiation. This is illustrated in Fig. 5 for two different laser pulse-widths. The effect of incubation is both modifying the absorbing cross-section through defect accumulation and inducing new routes for energy deposition into the lattice besides the electron-phonon coupling. Defects act like trapping centers strongly coupled to the lattice.

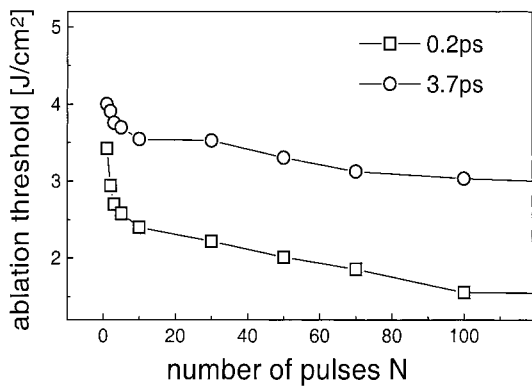


Fig. 5. Reduction of threshold fluence for ablation of sapphire (signaled by a burst in ion emission) as a function of preceding laser shots of the same fluence, documenting incubation. Two different pulse durations are examined, reflecting the well known^{4,8)} reduction of threshold fluence as the pulse width is reduced.

Velocity distribution of ejected particles (*in situ*)

In order to gain further insight into the nature of the gentle and strong ablation phases we have also measured the velocity distributions of the emitted particles by a time-of-flight analysis (TOF) of the particles ejected during each laser shot. A schematic overview of the experimental set-up is shown in Fig. 6.

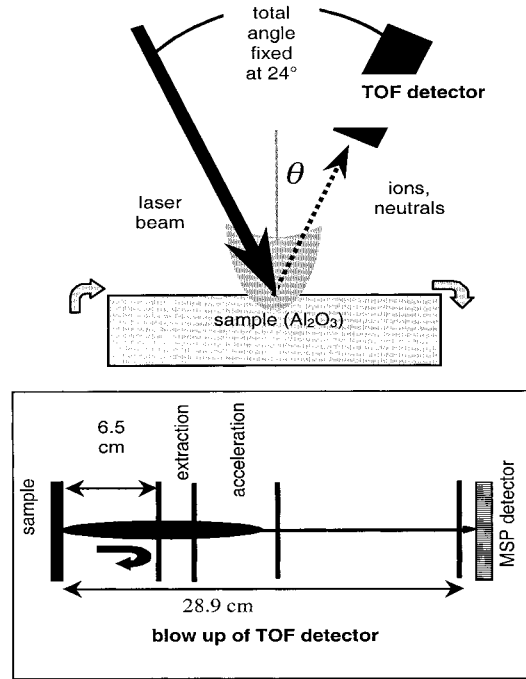


Fig. 6. Schematic of the experimental setup used to determine the angular and velocity distributions of the ablated particles.

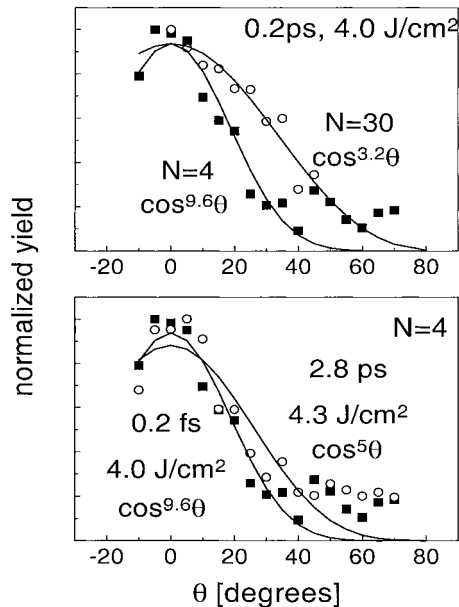


Fig. 7. Angular distribution of the ejected ions in the plume for three different sets of laser parameters. Experimental points are given by circles and squares, the $\cos^m\theta$ fits are given by full lines.

The target can be rotated around an axis perpendicular to the detection plane so that also angular distributions (θ dependence) of the ablated particles can be determined. The time-of-flight spectrometer (TOF) is a modified Wiley-McLaren setup, which can be operated such that both the masses and the velocities of the particles may be determined. This is illustrated in the lower panel of Fig. 6. By letting the ions drift over several cm into a pulsed extraction field the velocity is derived from the time between laser pulse being fired and the extraction field being applied. The measured time-of-flight spectra are projected onto a velocity scale thereby accounting for the appropriate Jacobian factor.

Two characteristic angular distributions measured with this set-up are shown in Fig. 7. We see that the distributions are strongly forward peaked, indicating efficient repulsion from the surface while for a purely thermal, statistical emission we would expect a $\cos\theta$ distribution from the laser irradiated spot (although, hydrodynamical effects in the plume will act towards narrowing). We also observe that higher number of shots and longer pulse lengths lead to broader distributions.

More information can be obtained from the velocity distributions, of which two characteristic examples are shown in Fig. 8 (TOF axis normal to the target).

We see distributions with most probable velocities of 20 to 50 km/s, which are far above thermal energies. They are particularly high in the region of gentle etching while the most striking feature observed is a dramatic shift towards lower velocities and also some broadening with increasing number of shots N . The same is observed for larger fluences as well as for increased pulse-widths. Generally speaking, the shift occurs at laser parameters for which in the ex-situ studies we have observed the transition from the gentle to the strong etch phase.

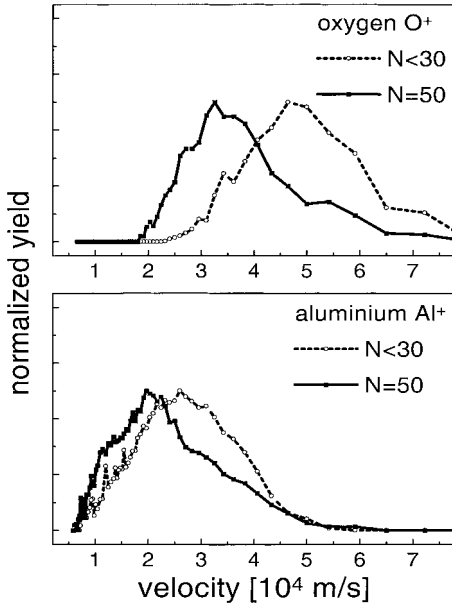


Fig. 8. Some examples of measured velocity distributions of the ions ejected from $c\text{-Al}_2\text{O}_3$ irradiated by 200 fs, 4 J/cm^2 laser pulses. The most probable velocity stays approximately constant for $N < 30$ and shifts drastically for larger N towards lower velocities as the strong ablation phase is reached.

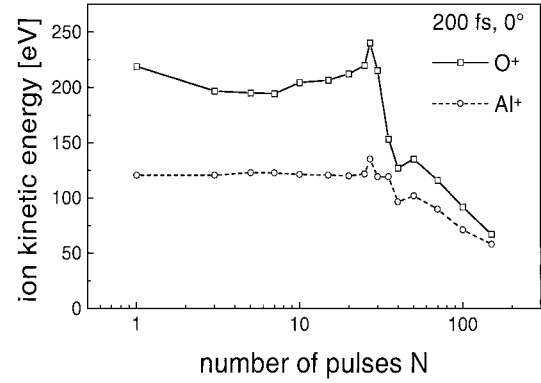


Fig. 9. Average kinetic energies of Al^+ and O^+ ions ejected normal to the $c\text{-Al}_2\text{O}_3$ surface irradiated by 200 fs, 4 J/cm^2 laser pulses as a function of the number of laser shots. At a small number of shots Al^+ and O^+ ions have different energies. Note the dramatic drop of energy at around $N \approx 30$ where the transition from gentle to strong etching occurs.

Figure 9 summarizes some of the data obtained for O^+ and Al^+ velocity distributions. We plot the ion average kinetic energy as a function of the number of laser shots for one set of laser parameters. We note that the kinetic ion energies observed are far above any reasonable assumption for a purely thermal origin, even in the strong ablation phase. It is, however, interesting to note that the energy of aluminium and oxygen atoms tends to become equal with a high number of shots, *i.e.* in the strong ablation phase, while they are distinctively different in the gentle ablation phase.

To illustrate this even more clearly, we show these data again in Fig. 10, this time in terms of the ratio between most probable momenta for the O^+ and Al^+ ions.

It is evident that the momenta of the ions are equal in the gentle etch phase compared to the strong etch phase, where, as pointed before, there is a tendency towards equal energies for both species. This observation give strong evidence that electrostatic forces (Coulomb explosion) dominate the gentle etch phase. If these act for a limited time (the average expulsion time t_{ex}) both ions (having the same charge q) experience the same electric force $F_{\text{El}}(t) = eE(t)$ in the space charge field $E(t)$ and we expect them to gain the same mo-

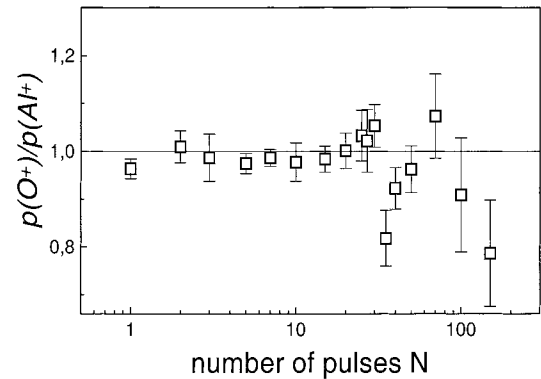


Fig. 10. Ratio of characteristic most probable momenta from measured velocity distributions of O^+ and Al^+ ions.

mentum:

$$p = \int_0^{t_{\text{ex}}} F_{\text{el}}(t) dt. \quad (1)$$

As a crucial check we can study doubly charged ions which should have twice the momentum of singly charged ions. This is indeed the case (not shown here^{9,10}).

For further argumentation we compare in Fig. 11 the Al^+ ion velocity distributions from Al_2O_3 and from metallic aluminium. These distributions were measured for $N = 2$ laser shots for sapphire and $N = 4$ for Al metallic sample and normalized to the individual maximum intensity in the following experimental conditions: 200 fs pulse duration and 4 J/cm^2 for sapphire, respectively 1.1 J/cm^2 for the metallic sample (both fluences being slightly above the ablation threshold for the respective materials). As clearly evidenced for Al^+ originating from dielectric sapphire the velocity distribution shows a quasi-bimodal structure, with a fast peak (energies above 100 eV, depending on the emission angle) followed by a slow peak (less than 50 eV). However, the Al^+ ions from the metal only show the low velocity distribution, similar to that observed from the dielectric after the onset of the “strong” ablation phase, with high abundance in the “thermal” region of the distribution. The velocity distributions for the dielectric and metallic sample are measured under comparable conditions, *i.e.* at fluences slightly above the ablation threshold.

It is important to note that the high kinetic energies of the fast peak (sapphire sample) explained in terms of Coulomb explosion are characteristic only for dielectrics, due to the poor electric transport properties. The slow neutralization

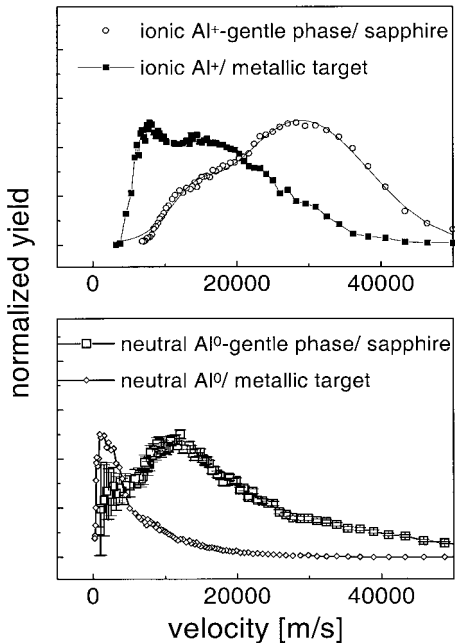


Fig. 11. Velocity distributions for Al^+ ions (upper panel) and neutrals (bottom panel) from Al_2O_3 (200 fs, $N = 2$, $F = 4 \text{ J/cm}^2$) and from aluminium metallic target (200 fs, $N = 4$, $F = 1.1 \text{ J/cm}^2$). TOF axis normal to the target.

of the uncompensated positive charge induced by photoemission will allow the surface neutrality breakdown to exist long enough for an electrostatic break-up of the surface. For metals, due to the efficient electron transport from the bulk, the conditions for a Coulomb explosion process are not met. The less energetic ions of the second peak (for the dielectric sample) will tentatively be attributed to a thermal process, which, especially in the strong etch-phase, resembles phase explosion.⁶⁾

Without going into details here we briefly mention that we have also measured the velocity of the neutral particles expelled from the irradiated area by using a second, post-ionizing time delayed XeCl excimer laser at 308 nm in the extraction zone and repelling the original ions before post-ionization.⁹⁾ The number of secondary ionized particles are proportional to the number of neutrals present in the extraction region within the focal spot of the XeCl excimer laser. We recall that these neutrals constitute 90% of the matter ablated in the gentle and 99% in the strong etch phase. This indicates a thermalisation process after the initial ionization phase from which only the fast Coulomb explosion ions can escape.

Obviously in Fig. 11, for sapphire, the neutrals arrive much later in the plume in comparison to the early, fast ions from the primary non-thermal, electrostatic mechanism. They have velocities characteristic of the thermal region in the ion velocity distribution, resembling that of the positive ions in the strong etch phase. This indicates a thermalisation process after the initial ionization phase, from which only the fast and previously emitted Coulomb explosion ions can escape. Small differences have been observed between gentle and strong phases for the dielectric case (not shown in the figure), but the most probable velocity of Al neutrals from the sapphire target is much higher than the corresponding velocity of the Al neutrals from a metallic Al target (comparison can be made since the laser fluences are in similar relation to the threshold values). This suggests that the temperatures are greatly increased for the laser irradiated dielectrics above the ablation threshold, approaching the critical temperature. No absolute temperature measurements are available but the experimental facts provide evidence for heating to extreme temperatures. Small clusters of material arriving later in the second-ionization region can play also a role in the low velocity tails of the distributions (especially for the metallic sample or in the conditions of the strong phase for the dielectric case).

Additional insight into the processes occurring during the initial phase of ablation is gained from detecting the emitted electrons and estimating their energy. This can be done by essentially reversing the electric potentials of our TOF spectrometer and negatively biasing the sample. Since the mass spectrometer was not designed for this purpose the energy resolution is rather poor.

Figure 12 shows the result of this experiment. It still gives us a very useful overview of what is happening: Clearly, two groups of electrons can be discerned: a very fast distribution arriving at the MSP at times less than a μs , corresponding to several eV of kinetic energy followed by a very slow group of ejected electrons with energies in the range of meV

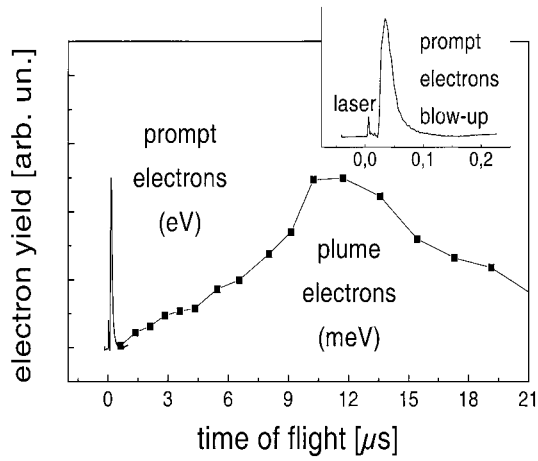


Fig. 12. Time-of-flight measurement for the electrons ejected during the gentle phase for 100 fs irradiation.

(the two distributions are normalized to individual maxima). Obviously, the first group reflects – at least part of – the initially emitted photoelectrons. They originate from direct multiphoton ionization of the valence band and defect states and from additional laser interaction with the free electrons in the conduction band.¹¹⁾ They leave the sample at an early time, which leads to the original build-up of the surface charge. The broad distribution of rather slow electrons is characteristic for the electrons that are simply carried along with the plume and help to partially neutralize the latter as it expands.

Additional evidence for the electrostatic origin of the initial surface break-up in the gentle etch phase comes from a semi-quantitative argument. The minimum charge density at the surface necessary to induce Coulomb explosion can simply be estimated from the requirement of electrostatic stress (force per unit area) to overcome the local mechanical (or bonding) stress¹²⁾:

The average electric stress (effective area per particle $S = \pi a_0^2/4$) is given by

$$\sigma_{\text{El}} = \frac{F_{\text{El}}}{S} = \frac{f^2 e^2 l}{\pi^2 \epsilon \epsilon_0 a_0^4}, \quad (2)$$

when a fraction f of the particles is ionized in the irradiated volume. Here a_0 is the average atomic spacing in the lattice (2 Å), $l = 3.64$ is a factor taking into account the lattice geometry and $\epsilon \approx 10$ the relative dielectric constant for sapphire. For the bulk material the mechanical stress $\sigma_{\text{Mech}} = (\Delta x/x)E$ for bond breaking has been estimated by $E/10$ where E is Young's modulus (335 GPa for sapphire¹³⁾). For atoms in the surface layer this will obviously be smaller and we take a compromise value of $E/20$. With these values we obtain $f \geq 0.5$ as the critical fraction of ionized species on the surface of the irradiated volume at which surface break-up due to Coulomb explosion is expected to occur.^{10,14)}

On the other hand, we may also obtain an estimate for f from the experimentally observed (most probable) momenta p of the ions above the threshold. With Eq. (1) we derive an average electric force assuming an effective expulsion time of 1 ps (the time scale during which the surface charge remains stable as evidenced by the pump-probe experiments described in

the next section). From the average electric force we derive finally *via* Eq. (2) $f = 0.6-0.8$, in good agreement with the former estimate.

From all these observations we conclude, that Coulomb explosion is indeed a dominant driving mechanism for ion expulsion during the gentle ablation phase. It is most directly seen in the momentum distribution of the ejected ions.

Pump-probe measurements

Finally, we report briefly about dynamical studies using femtosecond pump-probe techniques, which allows us to follow the dynamics of the energy deposition and redistribution process in real time. The experimental set-up is essentially unchanged, except that now we use two laser pulses which are delayed with respect to each other by a variable delay time Δt . Each of these pulses has a fluence below the single shot ablation threshold while both together are sufficient to overcome this value. By exposing the sample subsequently to both of these pulses, we can detect the energy redistribution channels within the sample. The key question here is how long the material remembers that it has been pre-treated by the pump pulse.

Figure 13 shows the fast ion Al^+ yield (20,000 m/s) when the sample is irradiated by a first sub-threshold 80 fs pulse and probed with a second, identical pulse, delayed by Δt . Several distinct features have to be distinguished, all of them clearly reproducible.

- i) The maximum observed at zero delay and the corresponding minimum at 0.1 ps between pump and probe pulse simply reflects the optical interference between the two coherent pulses of equal wavelength and is without relevance for the understanding of the ablation process.
- ii) After an initial decrease the signal rises to a first maximum and then decreases again, reaching a minimum at around 1 ps. We take this to reflect the initial electron dynamics and electrostatic energy accumulation at the surface. A hot electron bath and a sub-critical charge are initiated by the pump pulse. The second pulse adds to this excita-

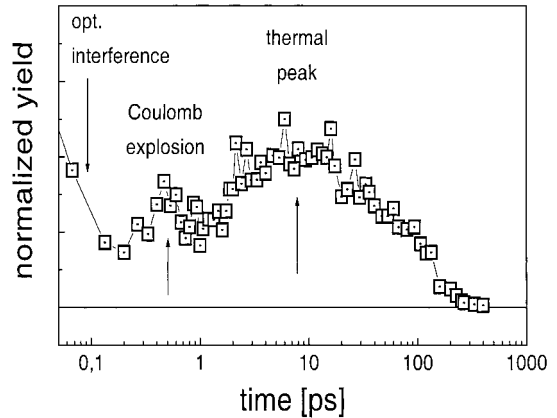


Fig. 13. Fast Al^+ ion signal in a pump-probe ablation measurement on sapphire with 80 fs pulse-width.

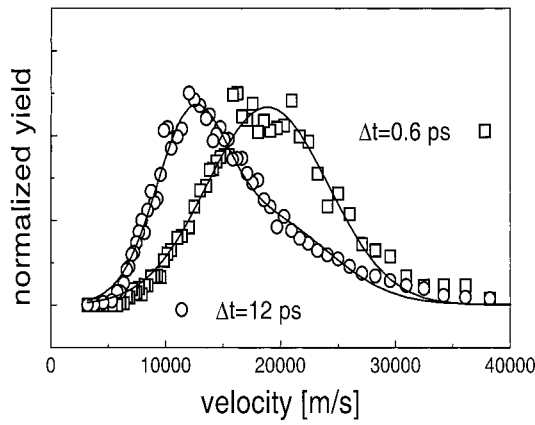


Fig. 14. Measured Al^+ ion velocity distributions at two different delay times Δt between pump and probe pulse marked by arrows in Fig. 13. Squares: $\Delta t = 0.6$ ps (Coulomb explosion), circles $\Delta t = 12$ ps (thermal origin). Same conditions as in Fig. 13.

tion, the threshold is exceeded and ion ejection occurs. The surface charge build-up is reflected by the maximum around 600 fs followed by decay after 1 ps, which we take as the time period necessary for the surface charge to survive at sufficient magnitude to lead to Coulomb explosion as discussed before. The following decay up to 1 ps reflects charge reduction, connected with the emission of charged particles and with neutralization due to carrier diffusion.

iii) The second rise of the ion signal is attributed to lattice heating due to electron-phonon coupling. In a separate experiment⁹⁾ we were able to detect increased optical scattering regarded as the onset of efficient ablation, *i.e.* the main, neutral component removal on the same time scale. Support of this interpretation is obtained from measuring the velocity distributions of the ions at the two different delay times marked in Fig. 13. This measurement is presented in Fig. 14. We see very clearly that at short delay time (< 1 ps) between pump and probe pulse the ion velocity replicates the fast ion distribution which we have observed in the gentle etch phase (scaled down to lower fluences) and which we attributed to Coulomb explosion. The dynamics involved in fast ion formation obviously relies on the availability of sufficient electron density in the conduction band to in-

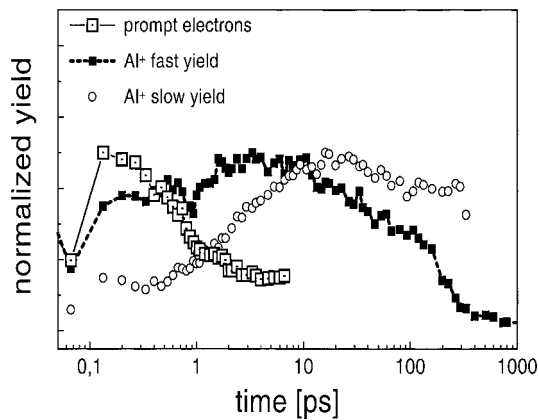


Fig. 15. Prompt electrons (empty squares) and fast (full squares) and slow (open circles) Al^+ ion signal in a pump-probe measurement on sapphire with 100 fs pulse width.

duce efficient photoemission and subsequent charging with IR pulses. In contrast, at long delay times (> 10 ps) electron energy has been transferred into the lattice so that a strong thermal process becomes effective and absorption of the second laser pulse couples better with the heat bath of the lattice.

In a second pump-probe experiment we have studied the response of the prompt electrons and compared it to the ion yield as illustrated in Fig. 15 (100 fs pulse duration). The electron signal follows the same temporal characteristics as the ion signal we have attributed to Coulomb explosion (the decay at around 1 ps in Fig. 13), supporting the idea of electrostatic ion ejection due to efficient photoemission.¹⁰⁾ Also, measuring the slow ion yield (12,000 m/s) we record the signature of a pure thermal effect on the time scale of electron-phonon coupling.

Conclusion

We have shown that the transition from the gentle to the strong etch phase in ultrashort laser ablation of wide band-gap materials, here exemplified by $c\text{-Al}_2\text{O}_3$, is closely related to the incubation process and can be explored in a quantitative manner. The gentle phase is connected with macroscopic surface break-up due to Coulomb repulsion and efficient emission of fast ions (10% of the total material emitted). At higher fluence and a larger number of laser shots a transition to the strong etch phase is observed, accompanied by a reduction of the degree of ionization (to about 1%) a drastic increase of the ablation rate and reduction of ion energy which goes along with a quasi thermalisation of the emitted particles. Pump-probe experiments allow us to follow the time evolution of the energy deposition and redistribution process and the balance between electrostatic energy accumulation and heat deposition. Surface charging is found to survive beyond the critical value for break-up for about 1 ps. Probe absorption is maximized first at about 600 fs due to better coupling with the hot electron system. Subsequently at about 10 ps, the time scale of electron-phonon thermalisation, the lattice appears to be most susceptible to couple to the probe photons as a consequence of temperature increase. Finally, after several 100 ps the sample has cooled and loses the intermediate ability for very efficient energy absorption. For further details we refer the interested reader to forthcoming publications.

We wish, however, to indicate some potential applications of the present findings which are subject to further studies in our laboratory: Lattice heating by the first pulse and efficient coupling of a second pulse after some ten picoseconds might open new avenues to overcome the well known difficulties with deep hole drilling into transparent materials or surface polishing in precision optics fabrication. Cracks, which are observed even with femtosecond lasers, could possibly be avoided when ablation in the gentle phase regime is combined with energy deposition into the premolten material by a second pulse.

Partial support of this work through BMBF contract 13N7048/7 is gratefully acknowledged.

References

- 1) H. Varel, D. Ashkenasi, A. Rosenfeld, R. Herrmann, F. Noack, and E. E. B. Campbell: Appl. Phys. A **62**, 293 (1996).
- 2) E. E. B. Campbell, D. Ashkenasi, and A. Rosenfeld: *Lasers in Materials Science* (Transtech Publications, Zurich-Uetikon, 1999).
- 3) A. C. Tam, J. L. Brand, D. C. Cheng, and W. Zapka: Appl. Phys. Lett. **55**, 2045 (1989).
- 4) D. Ashkenasi, A. Rosenfeld, H. Varel, M. Wahmer, and E. E. B. Campbell: Appl. Surf. Sci. **120**, 65 (1997).
- 5) B. C. Stuart, M. D. Feit, A. M. Rubenchik, B. W. Shore, and M. D. Perry: Phys. Rev. Lett. **74**, 2248 (1995); A.-C. Tien, S. Backus, H. Kapteyn, M. Murnane, and G. Mourou: Phys. Rev. Lett. **82**, 3883 (1999).
- 6) R. Kelly and A. Miotello: Appl. Surf. Sci. **96**, 205 (1996).
- 7) L. V. Zhigilei, P. B. S. Kodali, and B. J. Garrison: Chem. Phys. Lett. **276**, 269 (1997).
- 8) R. Stoian, H. Varel, A. Rosenfeld, D. Ashkenasi, E.E.B. Campbell, and R. Kelly: Appl. Surf. Sci. **165**, 44 (2000).
- 9) R. Stoian, D. Ashkenasi, A. Rosenfeld, and E. E. B. Campbell: Phys. Rev. B **62**, 13167 (2000).
- 10) R. Stoian, D. Ashkenasi, A. Rosenfeld, and E. E. B. Campbell: unpublished.
- 11) Ph. Daguzan, S. Guizard, K. Krastev, P. Martin, and G. Petite: Phys. Rev. Lett. **73**, 2352 (1994).
- 12) R. L. Fleischer, P. B. Price, and R. M. Walker: J. Appl. Phys. **36**, 3645 (1965).
- 13) D. R. Lide: *Handbook of Chemistry and Physics* (CRC Press, Boca Raton, 1993).
- 14) R. Stoian, D. Ashkenasi, A. Rosenfeld, M. Wittmann, R. Kelly, and E. E. B. Campbell: Nucl. Instrum. Methods Phys. Res. B **166/167**, 682 (2000).